doi:10.1111/j.1558-5646.2010.01168.x

COMPLEX EVOLUTIONARY TRANSITIONS AND THE SIGNIFICANCE OF C_3–C_4 INTERMEDIATE FORMS OF PHOTOSYNTHESIS IN MOLLUGINACEAE

Pascal-Antoine Christin,[1,2,3] Tammy L. Sage,[4] Erika J. Edwards,[1] R. Matthew Ogburn,[1] Roxana Khoshravesh,[4] and Rowan F. Sage[4]

[1]Department of Ecology and Evolutionary Biology, Brown University, 80 Waterman St, Box G-W, Providence, Rhode Island 02912

[2]Department of Ecology and Evolution, Biophore, Quartier Sorge, University of Lausanne, 1015 Lausanne, Switzerland

[3]E-mail: pascal-antoine_christin@brown.edu

[4]Department of Ecology and Evolutionary Biology, University of Toronto, 25 Willcocks Street, Toronto, Ontario M5S3B2, Canada

Received June 11, 2010
Accepted October 3, 2010

C_4 photosynthesis is a series of biochemical and structural modifications to C_3 photosynthesis that has evolved numerous times in flowering plants, despite requiring modification of up to hundreds of genes. To study the origin of C_4 photosynthesis, we reconstructed and dated the phylogeny of Molluginaceae, and identified C_4 taxa in the family. Two C_4 species, and three clades with traits intermediate between C_3 and C_4 plants were observed in Molluginaceae. C_3–C_4 intermediacy evolved at least twice, and in at least one lineage was maintained for several million years. Analyses of the genes for phosphoenolpyruvate carboxylase, a key C_4 enzyme, indicate two independent origins of fully developed C_4 photosynthesis in the past 10 million years, both within what was previously classified as a single species, *Mollugo cerviana*. The propensity of Molluginaceae to evolve C_3–C_4 and C_4 photosynthesis is likely due to several traits that acted as developmental enablers. Enlarged bundle sheath cells predisposed some lineages for the evolution of C_3–C_4 intermediacy and the C_4 biochemistry emerged via co-option of photorespiratory recycling in C_3–C_4 intermediates. These evolutionarily stable transitional stages likely increased the evolvability of C_4 photosynthesis under selection environments brought on by climate and atmospheric change in recent geological time.

KEY WORDS: **C_4 photosynthesis, complex trait, co-option, precondition, evolvability, evolutionary transitions.**

One aim of evolutionary biology is to understand how complex traits emerge during the diversification of organisms. The development of complex traits involves modification of multiple genes, a process thought to occur gradually. Successive steps in an evolutionary transition are difficult to reconstruct, but extant taxa with intermediate characters can help (Combes 2001; Lamb et al. 2007; Herron and Michod 2008; Ogawa et al. 2009). However, the evolutionary significance of these intermediate taxa must be evaluated in an appropriate phylogenetic framework to inform us about the evolution of a particular trait (Adoutte et al. 1999; Herron and Michod 2008).

C_4 photosynthesis is one of the best systems in which to study complex trait evolution. It has evolved at least 50 times in a wide range of flowering plants (Muhaidat et al. 2007), making it one of the most convergent of evolutionary phenomena. The function of C_4 photosynthesis is to enhance the efficiency of

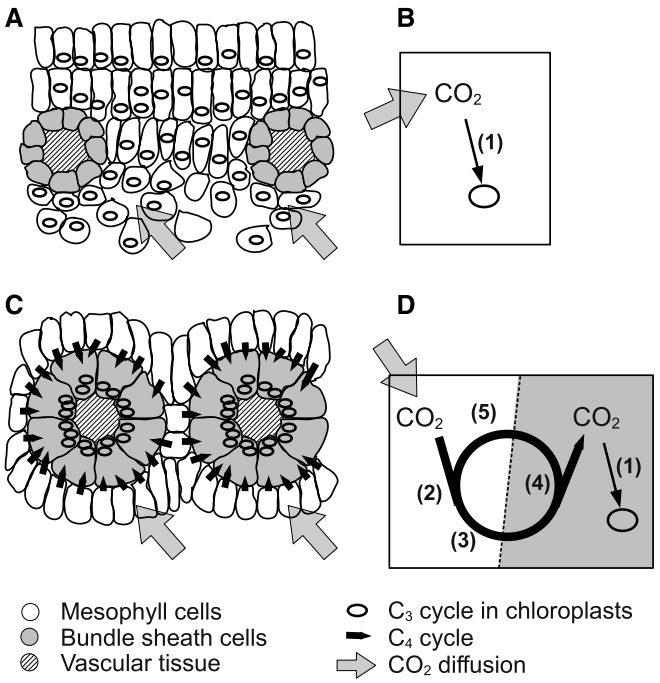

Figure 1. Anatomical and biochemical differences between C_3 and C_4 photosynthesis. These simplified diagrams present (A) the carbon assimilation in a C_3 leaf and (B) details of the biochemical steps in a mesophyll cell of a C_3 plant. By comparison, (C) carbon assimilation in a C_4 leaf involves important anatomical modifications and the addition of a biochemical pathway (black arrows), with (D) a close coordination of the biochemical steps between mesophyll and bundle sheath cells. Numbers in brackets represent the principal biochemical steps; 1 = fixation of CO_2 by Rubisco, which starts the Calvin cycle, 2 = fixation of CO_2 into an organic compound by a coupling of carbonic anhydrase and phosphoenolpyruvate carboxylase, 3 = transformation and transport of the organic compounds, 4 = release of CO_2 by one of the decarbxylating enzymes, 5 = regeneration of the carbon acceptors.

Rubisco, the primary CO_2 fixing enzyme in C_3 photosynthesis (Fig. 1). At current atmospheric conditions, Rubisco is significantly inhibited in warm climates by its ability to fix O_2 instead of CO_2, an inhibitory process termed photorespiration. C_4 plants overcome photorespiration by metabolically concentrating CO_2 into an inner cellular compartment where Rubisco is localized (Fig. 1). The C_4 concentrating mechanism arises from both morphological and biochemical innovations that function in unison to first fix CO_2 into organic compounds in the mesophyll tissue, and then to transport these compounds and release CO_2 into the chloroplasts of the cells that surround the vascular tissue (Fig. 1). These bundle sheath cells (BSC) are mainly involved in exchanges between veins and mesophyll in C_3 plants (Leegood 2008), but are responsible for CO_2 assimilation by Rubisco in C_4 plants (Fig. 1). Compared to C_3 plants, the typical C_4 foliar anatomy is characterized by large BSC surrounded by a low number of mesophyll cells, a reduction of the interveinal distance and an aggregation of chloroplasts in BSC (Fig. 1). These modifications allow a rapid exchange of metabolites between mesophyll cells and BSC and an efficient concentration of CO_2 from mesophyll to BSC. The kinetics and regulation of the enzymes used in the C_3 and C_4 cycles are also modified from ancestral forms, leading to a close coordination of the enzymes of each cycle (Leegood and Walker 1999; Engelmann et al. 2003; Hibberd and Covshoff 2010; Chastain 2011). Overall, dozens if not hundreds of genes have been modified during the evolution of C_4 plants from C_3 ancestors (Monson 1999; Sawers et al. 2007; Hibberd and Covshoff 2010).

How the C_4 pathway was repeatedly assembled in so many groups of flowering plants remains an open question. Hypotheses have focused on the successive acquisition of increasingly C_4-like characters in harsh environments induced by global climate change and reductions in atmospheric CO_2 content over the past 35 million years (Ehleringer et al. 1997; Sage 2004). The development of these hypotheses has been assisted by the study of species that exhibit characteristics intermediate between C_3 and C_4 photosynthesis (Hattersley et al. 1986; Rajendru et al. 1986; Griffiths 1989; Monson and Moore 1989; Sage et al. 1999; McKown et al. 2005; Vogan et al. 2007). These C_3–C_4 intermediates are known from multiple independent plant lineages (Sage et al. 1999). In these plants, the degree of cellular and enzymatic rearrangements varies from being close to C_3 species to being similar to fully developed C_4 plants. The Asteraceae genus *Flaveria* stands out as having more C_3–C_4 species than any other genus, with approximately 12 intermediate species (Ku et al. 1991, 1996; McKown et al. 2005). *Flaveria* has thus become the principle model for inferring past transitional stages in the origin of both C_4 anatomy (McKown and Dengler 2007) and C_4 biochemistry (e.g., Nakamoto et al. 1983; Engelman et al. 2003; Svensson et al. 2003). Phylogenetic evaluation of the relationships between *Flaveria* species confirmed that C_3 photosynthesis is the ancestral condition to C_4 photosynthesis, and that C_4 characters were successively acquired until C_4 species emerged (McKown et al. 2005). However, *Flaveria* is but one of the numerous plant lineages where C_4 photosynthesis independently evolved. Multiple C_3 to C_4 transitions should be evaluated to assess the generality of patterns, and to identify characters that might predispose certain C_3 taxa to evolve the C_4 pathway (Marshall et al. 2007; Vogan et al. 2007). Most C_3–C_4 intermediate species are relatively restricted in terms of geographic distribution and floristic importance (Sage et al. 1999). However, two species, *Mollugo verticillata* (carpet weed) and *Mollugo nudicaulis* (John's Folly) are successful cosmopolitan weeds of disturbed areas in warm climates (Vincent 2003). *Mollugo verticillata* was the first discovered C_3–C_4 species (Kennedy and Laetsch 1974), and for many years, it has been assumed that this species was a close relative of the only C_4 species

known in the Molluginaceae, *Mollugo cerviana*. However, there has been no systematic survey of photosynthetic pathways in this family and a lack of sufficient phylogenetic information has prevented any analysis of the relationships between its C_3, C_3–C_4 and C_4 species. The few phylogenetic studies incorporating representatives of Molluginaceae indicate the group as traditionally circumscribed is likely polyphyletic (Cuénoud et al. 2002; Brockington et al. 2009).

In this study, we identify the photosynthetic pathway of over 100 species in the Molluginaceae sensu lato, and then address C_4 evolution in the family by examining leaf anatomy and reconstructing the evolutionary relationships between C_3 and C_4 species and taxa that exhibit intermediate traits between the two pathways. We adopted a dense, family-wide sampling, including multiple accessions from diverse geographic origins for several species, notably the C_4 and C_3–C_4 taxa. Phylogenetic hypotheses using plastid markers were integrated in a broader analysis of eudicots and time calibrated with information from numerous fossils. We also sequenced nuclear genes encoding phosphoenolpyruvate carboxylase (PEPC), a key enzyme of the C_4 pathway, to gain insights into the evolutionary optimization of C_4 biochemistry in the Molluginaceae. The combination of photosynthetic, anatomical, and molecular datasets enabled us to isolate some of the steps in C_4 evolution, and provides fertile new ground for developing hypotheses about anatomical and ecological conditions that promote the evolution of this complex trait.

Material and Methods

PLANT SAMPLING AND CARBON ISOTOPE RATIOS

We sampled extensively from as many species of the Molluginaceae sensu lato as possible, following the classification of Endress and Bittrich (1993). Dried samples from herbarium specimens were obtained from numerous botanical gardens and herbaria (Table S1). When available, multiple accessions per species were analyzed.

For each sample, approximately 2 mg of plant tissue (stem, roots or leaves) was assayed for carbon isotope ratio using an Integra mass spectrometer with a Pee Dee belamnite standard. Carbon isotope ratios were determined by the University of California stable isotope facility (http://stableisotopefacility.ucdavis.edu).

Most herbarium specimens were too degraded for DNA extraction and only a subset of the samples used for carbon isotope ratios were included in the phylogenetic analyses (Table S2).

ISOLATION OF PLASTID MARKERS

Genomic DNA (gDNA) was extracted using the DNeasy Plant Mini Kit (Qiagen, GmbH, Germany) following the provider recommendations. Two plastid markers were selected for phylogenetic reconstruction, the coding gene *rbcL* and the region encompassing *trnK* introns and *matK* coding sequence. For accessions that yielded good quality DNA, each of these markers was amplified in a single polymerase chain reaction (PCR), using primers designed in this study based on sequences available in GenBank. Primers for *rbcL* were *rbcL_4_For* TCACCACAAACAGARACTAAAGC and *rbcL_1353_Rev* GCAGCNGCTAGTTCAGGACTC. They amplify a 1326-bp fragment, which represents 93% of the whole coding sequence. For *trnK-matK*, the primers were *trnKmatK_For* AGTTTRTMAGACCACGACTG and *trnKmatK_Rev* GCACACGGCTTTCCCTATG. They amplify a 2260–2420 segment, depending upon the species that comprises the whole coding sequence of *matK* and intron regions of *trnK*. PCRs were carried out in a total volume of 50 μl, including about 100 ng of gDNA template, 10 μl of 5× GoTaq Reaction Buffer, 0.15 mM dNTPs, 0.2 μM of each primer, 2 mM of $MgCl_2$, and 1 unit of *Taq* polymerase (GoTaq DNA Polymerase, Promega, Madison, WI). For *rbcL*, the PCR mixtures were incubated in a thermocycler for 3 min at 94°C followed by 37 cycles consisting of 1 min at 94°C, 30 sec at 48°C and 90 sec at 72°C. This was followed by 10 min at 72°C. The PCR conditions were similar for *trnK-matK* except that annealing temperature was set to 51°C and the extension time to 2 min 30. Successful amplifications were purified using the QIAquick PCR Purification Kit (Qiagen) and sequenced with the Big Dye 3.1 Terminator Cycle Sequencing Kit (Applied Biosystems, Foster City, CA), following the provider instructions, and separated on an ABI Prism 3100 genetic analyzer (Applied Biosystems). For *rbcL*, two internal primers were used; *rbcL_629_For* CRTTTATGCGTTGGAGAGACC and *rbcL_760_rev* CAAYTCTCTRGCAAATACAGC. Sequencing of *trnK-matK* was first performed with the *trnKmatK_For* primer and internal primers were then designed based on the partial sequences obtained (Fig. S1).

For most samples, the gDNA obtained were too degraded to amplify long fragments of DNA. The gDNA of species that failed the amplification of full *rbcL* or *trnK-matK* were used as a template to amplify short overlapping fragments, with a battery of internal primers designed for this study (Fig. S1). The size of targeted fragments was reduced, until PCR succeeded, to 200 bp for some gDNA. PCR reactions were run as described above for *rbcL* except that the extension time was lowered to 45 sec. Purifications and sequencing were performed as described above, but one of the PCR primers was used for sequencing reaction.

PHYLOGENETIC ANALYSES

The GenBank database was screened and Caryophyllales species for which both *rbcL* and *matK* or *trnK-matK* were available were added to the dataset. In addition, species from other eudicot lineages, one taxon from the eudicot sister group (Ceratophyllales) and one monocot (*Acorus americanus*; used as outgroup) were added from GenBank to allow more calibration points to be used

in the molecular dating analyses (see below; Table S3). Sequences were aligned using ClustalW (Thompson et al. 1994) and the alignment was manually refined. Phylogenetic trees were then inferred using a Bayesian procedure implemented in MrBayes 3.1 (Ronquist and Huelsenbeck 2003). The noncoding introns of *trnK* were very difficult to align between species from different families. Therefore, only *rbcL* and *matK* were considered for species outside Molluginaceae sensu stricto (hereafter referred to as Molluginaceae), these coding genes being unambiguously aligned. These two markers were analyzed separately and in combination, to check for congruence. The noncoding *trnK* introns were included only for Molluginaceae, after the alignment was manually refined. These species being more closely related, the alignment of *trnK* was not problematic.

The substitution model was set to a general time reversible model with a gamma shape distribution and a proportion of invariant sites (GTR + G + I), as identified as the best-fit model by hierarchical likelihood ratio tests (hLRT). Two Bayesian analyses, each of four parallel chains, were run for 10,000,000 generations. A tree was sampled each 1,000 generations after a burn-in period of 3,000,000 generations. A consensus tree was computed from the 14,000 sampled trees.

The obtained phylogeny was used for molecular dating using a Bayesian method that accounts for changes in rates of evolution among branches, following the recommendations of Rutschmann (2006). The *trnK* marker was not used in the dating analyses. Model parameters were estimated with baseml (Yang 2007) for the two genes separately. Branch lengths and the variance–covariance matrix were then optimized using estbranches (Thorne et al. 1998). A Bayesian Markov chain Monte Carlo (MCMC) procedure implemented in multidivtime (Kishino et al. 2001; Thorne and Kishino 2002) approximated the posterior distributions of substitution rates and divergence times, given a set of time constraints. The MCMC procedure was run for 1,000,000 generations after a burn-in of 100,000 generations, with a sampling frequency of 100 generations. The outgroup (*A. americanus*) was removed during the analysis. The maximal age for the root of the tree was set to 160 million years ago (Mya), a time that generally exceeds estimates of monocot–eudicot divergence (Magallon and Sanderson 2001; Friis et al. 2006), and nine different constraints were set on internal nodes. The first evidence of eudicots in the fossil record comes from tricolpate pollen, which appeared during the late Barremian and early Aptian (Magallon and Sanderson 2001; Friis et al. 2006). This was used to set a lower bound of 120 Mya to the stem group node and an upper bound of 130 Mya to the crown group node of eudicots. This upper bound assumes that the time span between the emergence of eudicots and their fingerprint in the fossil records does not exceed a few million years. Lower bounds were set to the stem group nodes of several eudicot orders following Magallon and Sanderson (2001): 102.2 Mya for Buxales, 91.2 for Malpighiales, 59.9 for Fabales, 69.7 for Malvales, 88.2 for Myrtales and 91.2 for Ericales. In addition, a lower bound of 34 Mya was set to the divergence of *Polycarpon* and the higher Caryophyllaceae (here represented by *Silene*, *Schiedea* and *Scleranthus*), according to the phylogenetic position of a fossil reported by Jordan and Mcphail (2003). The same analysis was rerun excluding successively each calibration point to check for major incongruence among constraints, and also rerun without the upper bound on the crown of eudicots and using a maximum age of the root of 200 Mya, to take into account recent analyses suggesting that Angiosperms may be older than previously thought (Smith et al. 2010).

ANALYSES OF GENES ENCODING PEPC

Genes encoding phosphoenolpyruvate carboxylase (*ppc*) of eudicot species were retrieved from GenBank. These were aligned and used to design a pair of primers theoretically able to amplify all Caryophyllales *ppc*; *ppc-1294-For* GCNGATGGAAGYCTTCTTG and *ppc-2890-Rev* GCTGGNATGCAGAACACYG. The forward primer is located in exon 8, whereas the reverse primer extends to the stop codon in exon 10. The amplified region is homologous to the gene portion previously studied in grasses (Christin et al. 2007) and sedges (Besnard et al. 2009) and which contains major determinants of the C_4 function (Bläsing et al. 2000; Jacobs et al. 2008). The studied fragment includes more than 1500 bp of coding sequence, which represents more than half of the full coding sequence.

The designed primers were used to PCR-amplify *ppc* genes from a subsample of the gDNA used for plastid markers and that were of good quality. About 100 ng of gDNA were mixed with 5 μl of 10× AccuPrime PCR Buffer, 0.2 mM of each dNTP, 0.2 μM of each primer, 3 mM of $MgSO_4$, 2.5 μl of DMSO and 1 unit of a proof-reading *Taq* polymerase (AccuPrime Taq DNA Polymerase High Fidelity, Invitrogen, Carlsbad, CA) in a total volume of 50 μl. The PCR mixtures were incubated at 94°C for 2 min, followed by 35 cycles consisting of 30 sec at 94°C, 30 sec at 51°C and 3 min at 68°C. The last cycle was followed by 20 min at 68°C. PCR products were run on a 0.8% agarose gel and purified with the QIAquick Gel Extraction Kit (Qiagen). Purified products were cloned into the pTZ57R/T vector using the InsT/Aclone PCR Product Cloning Kit (Fermentas, Vilnius, Lithuania). Up to 20 clones for each PCR product were amplified with *ppc-1294-For* and *ppc-2890-Rev* primers. The PCR products were restricted with the *Taq*I restriction enzyme (Invitrogen) and insert of each clone with a distinct restriction pattern was purified and sequenced as described for plastid markers. Sequencing reactions were performed first with the *ppc-1294-For* primer and then with internal primers.

Exons were identified through homology with the available *ppc* sequences and following the GT–AG rule. Coding sequences

were translated into amino acids and aligned using ClustalW (Thompson et al. 1994). Once translated back into nucleotide, the alignment was manually refined and used to infer a phylogenetic tree using MrBayes 3.1 (Ronquist and Huelsenbeck 2003). Eudicots and a sample of monocots *ppc* genes available in GenBank were added to the dataset (Table S4). The best-fit substitution model was determined through hLRT as the GTR + G + I. Bayesian analysis was run as described for plastid markers, but model parameters were estimated independently for first, second, and third positions of codons. Amino acids changes similar to those shown to be under positive selection for the C_4 function in Poales (Christin et al. 2007; Besnard et al. 2009) were reported on the phylogenetic tree.

ANATOMICAL ANALYSIS

Leaf sections from living specimens of *M. pentaphylla*, *M. verticillata*, *M. nudicaulis*, and *M. cerviana* were fixed in glutaraldehyde, postfixed in osmium, and embedded in Spurr's resin (Spurr 1969) as described by Sage and Williams (1995). In addition, because access to living species is often difficult, and the use of herbarium material to produce microimages of leaves would assist phylogenetic-based studies of photosynthetic pathway evolution, 18 accessions from Molluginaceae were sampled to assess variation in leaf anatomy (Table S2). Approximately 5 mm^2 of herbarium leaf samples were rehydrated in ddH_2O over night and subsequently fixed in 2% glutaraldehyde buffered with 0.05 M sodium cacodylate buffer (pH 6.9) for 24 h. Fixed samples were dehydrated in 10% ethanol increments and also embedded in Spurr's resin. All embedded leaf samples were sectioned at 1.5 μm, stained with toluidine blue-O in 0.2% benzoiate buffer (pH 4.4; O'Brien and McCully 1981), and imaged with a Zeiss Axioplan microscope (Carl Zeiss, Göttingen, Germany) equipped with an Olympus DP71 digital camera and imaging system (Olympus Canada, Markham Ontario).

Results

CARBON ISOTOPE RATIOS

A total of 314 accessions classified into 116 species from the Molluginaceae and affiliated taxa was typed for carbon isotope ratios. Values between −21‰ and −32‰ are indicative of C_3 species; values between −9‰ and −16‰ indicate C_4 species, whereas −16‰ to −19‰ indicate C_4-like species (von Caemmerer 1992). C_3–C_4 intermediate species normally have a C_3 isotopic ratio unless there is significant engagement of PEPC and a C_4 metabolic cycle as occurs in C_4-like species (von Caemmerer 1992). Only accessions from two Molluginaceae species, *M. cerviana* and *Mollugo fragilis*, exhibited C_4 carbon isotope ratios typical of C_4 plants (Table 1; Table S1). Although *M. cerviana* is known to be C_4 (Kennedy and Laetsch 1974), *M. fragilis* represents a newly discovered C_4 taxon. All other taxa had C_3 isotope ratios, including two taxa (*M. verticillata* and *M. nudicaulis*) previously demonstrated to be C_3–C_4 intermediates (Sayre and Kennedy 1979; Kennedy et al. 1980; Fig. S2).

PHYLOGENETICS AND DISCREPANCIES WITH TAXONOMY

Plastid markers were obtained for a total of 94 accessions, including 73 Molluginaceae and 46 *Mollugo*. Both *rbcL* and *trnK-matK* markers were completed for all but 15 accessions (Table S2). With 80 additional accessions retrieved from GenBank, the phylogenetic dataset contained 174 accessions labeled as 144 different species (Table 1). The phylogenies inferred separately from *rbcL* and *matK* were fully congruent with each other (data not shown). These coding markers were thus combined (Fig. 2). The family Molluginaceae as originally circumscribed (Endress and Bittrich, 1993) is polyphyletic, confirming results found with a limited species sampling (Cuénoud et al. 2002; Brockington et al. 2009). *Limeum* is sister to a large clade containing Molluginaceae and other families, justifying its treatment as a separate family (Limeaceae; APG III 2009). The Australian genus *Macarthuria* appears as the sister group of all other core Caryophyllales. *Corbichonia* and most *Hypertelis* are sister to a clade comprising Aizoaceae and Nyctaginaceae. Notably, one species of *Hypertelis* (*H. spergulacea*) falls within Molluginaceae (Fig. 3). The close relationship between *H. spergulacea* and *M. cerviana* inferred from plastid markers was also highly supported by two different nuclear genes (*ppc-1* and *ppc-2*; Fig. S3). The synonym *Mollugo linearis* auct. Non Ser. Em Dc. (Tropicos 2010) should possibly be resurrected for *H. spergulacea*. Molluginaceae are highly supported as the sister group of the Portulacineae clade (Nyffeler et al. 2008; Nyffeler and Eggli, 2010) and contain the genera *Mollugo*, *Adenogramma*, *Coelanthum*, *Glinus*, *Glischtrothamnus*, *Pharnaceum*, *Polpoda*, *Psammotropha*, and *Suessenguthiella*, and *H. spergulacea* (Figs. 2 and 3).

Within Molluginaceae, the phylogeny inferred from *rbcL* and *trnK-matK* is very well resolved, with most branches having a posterior probability of 0.99 or 1.0 (Fig. 3), and fully congruent with relationships deduced from the nuclear *ppc* genes (Fig. S3). *Mollugo* is not monophyletic, being largely mixed with the other Molluginaceae genera. The clade with the two C_4 species (*M. cerviana* and *M. fragilis*) and *H. spergulacea* is sister to a clade composed of diverse genera *(Adenogramma, Coelanthum, Mollugo*, *Pharnaceum, Polypoda, Psammotropha, Suessenguthiella)* originating mainly from southern Africa (Fig. 3). All members of this South African clade have C_3 isotopic ratios. The rate of molecular evolution of plastid markers was strongly accelerated in this region of the tree when compared to other eudicots, a pattern observed with both *rbcL* and *matK* (data not shown), but not with nuclear markers (Fig. S3). This phenomenon, which also occurred in the mitochondrial genome of some Geraniaceae and

Table 1. Carbon isotope ratios of species sampled for this study. C_4 and C_3–C_4 species are highlighted in bold. Numbers in parenthesis are sample size if greater than 1. See Table S1 for herbarium vouchers and raw isotope values.

	$\delta^{13}C$ (sample size)	Geographic region
Adenogramma		Confined to South Africa
A. capillaris	−30.7	South Africa
A. glomerata	−28.2 (4)	South Africa
A. lichtensteiniana	−26.8 (2)	South Africa
A. mullugo	−28.1 (3)	South Africa
A. rigida	−27.3	South Africa
A. sylvatica	−28.9 (3)	South Africa
Coelanthum		South Africa, SW Africa
C. grandiflorum	−25.8 (2)	South Africa, Namibia
C. parviflorum	−27.0	South Africa
C. semiquinquefidum	−24.7 (2)	South Africa Namibia
Corbichonia		southern Africa and Saudi Arabia
C. decumbens	−27.2 (3)	arid & semiarid Africa to SW Asia
C. rubriviolacea	−25.6 (2)	SW Africa
Corrigiola		
C. andina	−30.4	(sub)tropical South and central America
C. capensis	−28.2 (3)	tropical east Africa
C. drymaroides	−26.6 (2)	Malawi. Mozambique, Zimbabwe
C. litoralis	−28.1 (3)	temperate zones to subtropics, old world
C. paniculata	−27.0	Tanzania, Zambia
C. squamosa	−28.2	(sub)tropical South America
Glinus		pantropical to temperate zones
G. bainesii	−26.4 (3)	Zambia, Zimbabwe
G. herniarioides	−25.3	SE Asia
G. lotoides	−27.1 (10)	pantropical to temperate weed
G. oppositifolius	−28.4 (14)	sub-Saharan Africa to Australia
G. orygioides	−23.3	NE Australia
G. radiatus	−28.8 (7)	Americas, introduced to Africa
G. setiflorus	−26.2 (3)	Arabia, Kenya, Somalia, Tanzania
Glischrothamnus ulei	−28.0	Brazil
Hypertelis		southern Africa, Madagascar, St. Helena
H. angrae-pequenae	−25.5 (2)	South Africa, Namibia
H. arenicola	−26.6	South Africa
H. bowkeriana	−26.0 (5)	southern Africa, Kenya
H. ceaspitosa	−24.0	Namibia, South Africa
H. salsoloides	−25.1 (3)	southern Africa
H. spergulacea	−26.7 (2)	Namibia, South Africa
H. trachysperma	−25.6	South Africa
Limeum		southern Africa to south Asia
L. aethiopicum	−25.6 (9)	South Africa, Zimbabwe
L. africanum	−26.7 (2)	southern Africa
L. angustifolium	−27.7	Somalia
L. arabicum	−25.5 (2)	Arabian peninsula
L. arenicolum	−24.3 (2)	southern Africa
L. argute-carinatum	−25.0	southern Africa, Angola
L. deserticolum	−26.8	southern Africa
L. dinteri	−26.6 (3)	southern Africa
L. fenestratum	−27.2 (4)	southern subtropical Africa
L. glaberrimum	−26.2	Mozambique

Continued.

Table 1. Continued.

	$\delta^{13}C$ (sample size)	Geographic region
L. humifusum	−27.0	South Africa
L. linifolium	−24.9	South Africa
L. myosotis	−25.5 (2)	southern Africa, Angola
L. obovatum	−26.6 (2)	Sahara region to India
L. praetermissum	−28.3 (2)	Kenya, Somalia
L. pterocarpum	−28.1 (5)	subtropical Africa
L. rhombifolium	−25.7 (2)	Namibia, South Africa
L. sulcatum	−25.5 (4)	southern Africa
L. telephioides	−25.2	South Africa
L. viscosum	−26.4 (4)	subtropical, east-tropical Africa
Macarthuria		Australia
M. apetala	−26.5 (2)	Australia
M. australis	−27.0 (2)	Australia
M. complanata	−29.4	NE Australia
M. ephedroides	−28.5	NE Australia
M. neocambrica	−27.6 (2)	Australia
Mollugo		pantropical to temperate zones
M. angustifolia	−29.3	Somalia
M. cerviana	**−13.3 (19)**	hot arid regions, pantropics to temperate
M. crockeri	−26.5	Galapagos
M. decandra	−29.4 (3)	Madagascar
M. enneandra	−28.2 (2)	Cuba
M. flavescens	−25.5 (6)	Galapagos
M. f. subsp. *gracillima*	−27.0 (3)	Galapagos
M. f. subsp. *insularis*	−27.2	Galapagos
M. floriana	−25.5 (2)	Galapagos
M. fragilis	**−13.2 (3)**	Angola (coastal sand)
M. molluginis	−29.0 (6)	Australia
M. namaquensis	−27.4 (3)	South Africa
M. nudicaulis (C_3–C_4)	**−28.4 (10)**	pantropical and subtropical
M. nudicaulis var. navassensis	−29.7 (2)	Caribbean
M. pentaphylla	−28.8 (13)	pantropics and subtropics
M. pusilla	−28.5	Namibia, South Africa
M. racemosa	−27.4 (4)	India, Sri Lanka
M. snodgrassii	−25.3 (4)	Galapagos
M. tenella	−28.0 (5)	Namibia, South Africa
M. verticillata (C_3–C_4)	**−27.6 (12)**	cosmopolitan weed
Pharnaceum		southern Africa
P. albens	−26.9 (2)	Namibia, South Africa
P. brevicaule	−26.9	southern Africa
P. confertum	−27.4	South Africa
P. cordifolium	−27.8	South Africa
P. croceum	−25.2 (2)	Namibia, South Africa
P. detonsum	−26.5 (2)	South Africa
P. dichotomum	−27.3 (2)	South Africa
P. elongatum	−29.1 (2)	South Africa
P. exiguum	−27.9	South Africa
P. fluviale	−26.7	South Africa
P. incanum	−28.1 (3)	South Africa
P. lanatum	−28.2 (3)	South Africa

Continued.

Table 1. Continued.

	$\delta^{13}C$ (sample size)	Geographic region
P. lineare	−25.5 (2)	South Africa
P. microphyllum	−28.5	South Africa
P. reflexum	−27.8	South Africa
P. subtile	−27.2	South Africa
P. thunbergii	−32.0 (2)	South Africa
P. trigonum	−29.4	South Africa
P. verrucosum	−24.0 (4)	southern Africa
P. viride	−26.5	South Africa
P. zeyheri	−28.9	South Africa
Polpoda		South Africa
P. capensis	−24.9 (3)	South Africa
P. stipulacea	−25.2	South Africa
Psammotropha		southern to tropical Africa
P. alternifolia	−26.6	South Africa
P. anguina	−30.1	South Africa
P. frigida	−26.1	South Africa
P. mucronata	−27.4 (4)	Mozambique, South Africa
P. myriantha	−28.2 (2)	southern Africa
P. obovata	−24.3 (2)	South Africa
P. obtusa	−26.6	South Africa
P. quadrangularis	−28.1 (2)	South Africa
Suessenguthiella scleranthoides	−24.9 (2)	Namibia, South Africa
Telephium		Mediterranean basin and Arabian peninsula
T. barbeyanum	−28.2	Libya
T. imperati	−26.6 (2)	North Africa, Spain
T. orientale	−26.4	Turkey
T. oligopsermum	−27.2 (2)	Iraq
T. sphaerospermum	−27.6 (2)	Yemen
Trianthema		
T. portulacastrum	**−14.0**	
Zaleya		
Z. pentandra	**−12.4**	
Excluded		
Mollugo minuta	−24.0 (2)	South Africa
Pharnaceum cupitatum	−25.7	South Africa
Pharnaceum spergulacea	−24.9	South Africa
Psammotropha eriantha	−29.2	South Africa
Psammotropha rosularis	−28.0	southern Africa

Plantaginaceae (Cho et al. 2004; Parkinson et al. 2005), suggests a higher mutation rate, potentially due to the decrease of the quality of DNA replication and repair in the chloroplasts of some Molluginaceae. However, the grouping of these species cannot be attributed to long-branch attraction because they also share numerous unique insertions that represent synapomorphies (in particular, a 33 bp insertion in the coding sequence of *matK*).

The sampling of multiple accessions per species also revealed several *Mollugo* species that are not monophyletic—*M. cerviana*, *M. nudicaulis*, and *M. verticillata*. *Mollugo cerviana* is paraphyletic with respect to *M. fragilis* and *H. spergulacea* (Fig. 3). Two clades of *M. cerviana* include accessions from overlapping geographical ranges and are highly divergent in both plastid and nuclear markers (Fig. 3 and Fig. S3), suggesting they correspond to distinct species. The two *M. cerviana* clades will hereafter be referred to as the *cerviana* group (which includes old world and Australian *M. cerviana*) and the *fragilis* group (which includes old and new world *M. cerviana* as well as *M. fragilis*). This complex (*M. fragilis*, *M. cerviana* and *H. spergulacea*) requires renewed taxonomic attention. Biogeographic and population

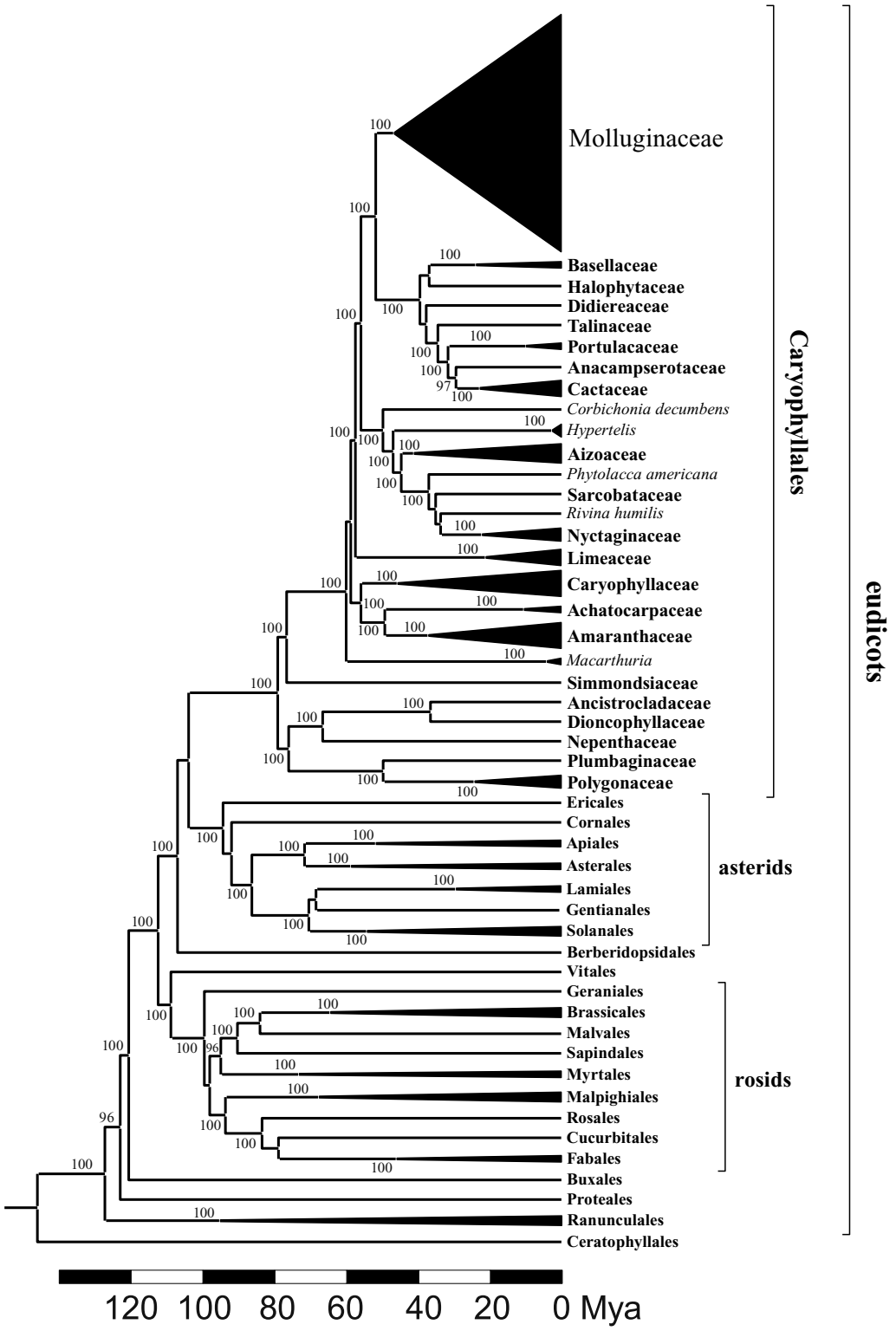

Figure 2. Dated phylogeny and position of Molluginaceae within eudicots. The topology was obtained through Bayesian inference of coding sequences from the plastid markers *rbcL* and *matK*, and *trnK* for Molluginaceae. Bayesian support values are indicated near branches when greater than 90. Branch lengths are proportional to estimated divergence times, in million years ago (Mya). This tree was rooted on monocots, which were removed during the dating analysis. Families of Caryophyllales and other orders are compressed, except for taxa with problematic taxonomic position, for which genus or species names are indicated. The part of the tree corresponding to Molluginaceae is detailed in Figure 3. Major groups are indicated on the right.

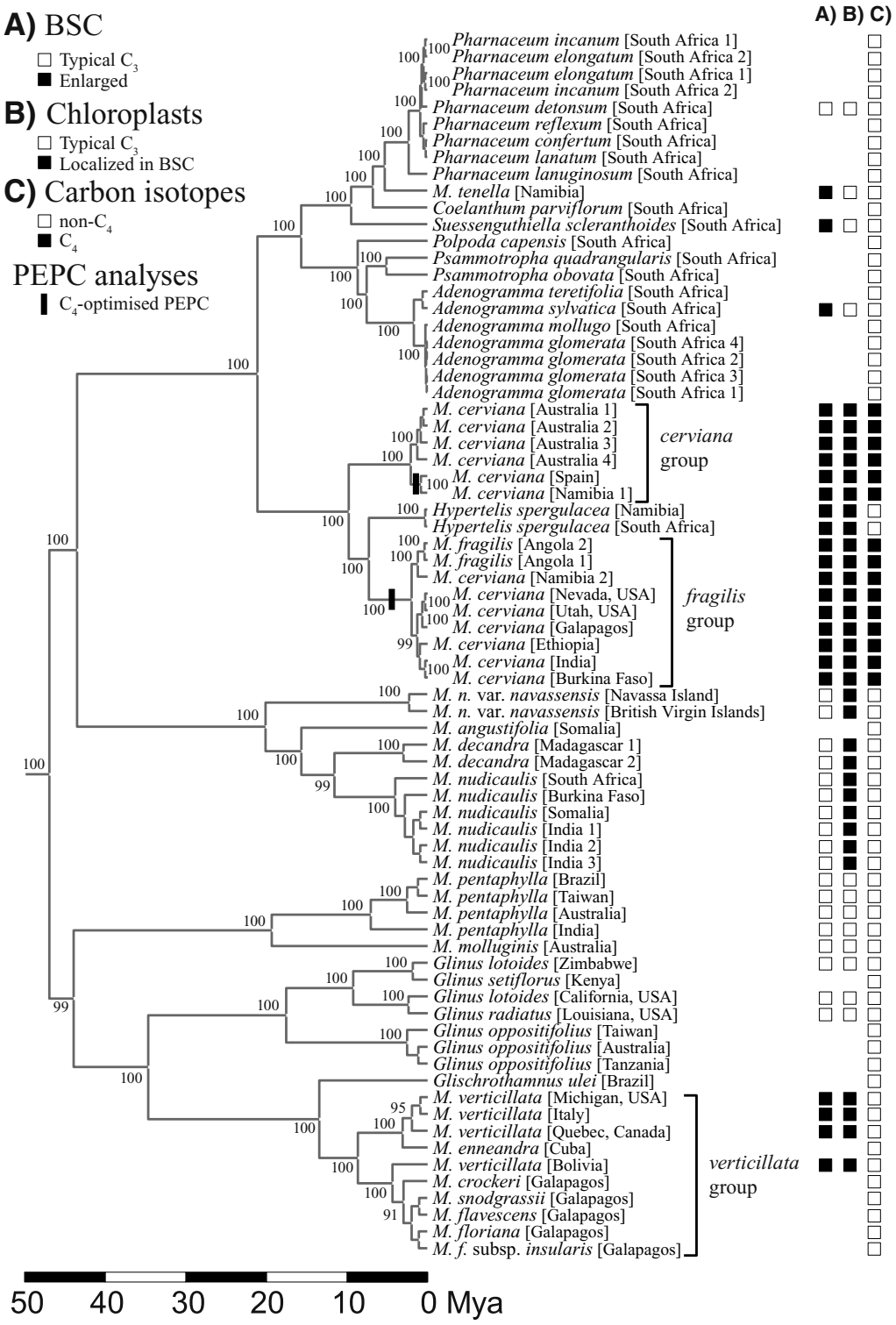

Figure 3. **Dated plastid phylogeny of Molluginaceae and photosynthetic types. This figure details the Molluginaceae part of Figure 2. Bayesian support values are indicated near branches when greater than 90. Branch lengths are proportional to estimated divergence times, in million years ago (Mya). Each accession name is followed by its geographical origin, in square brackets. Numbering is used to differentiate accessions from the same species and geographical origin. It corresponds to that in Table S2. Groups of accessions described in the text are delimited on the right. Squares represent indicators of photosynthetic types; (A) size of bundle sheath cells (BSC; white = typical C_3, black = enlarged), (B) localization of chloroplasts (white = typical of C_3 plants, black = aggregation in BSC) and (C) carbon isotopes ratio (white = non-C_4, black = C_4). Branches where PEPC was optimized for the C_4 function, as deduced from analyses of genes encoding PEPC (Fig. 5), are indicated by vertical bars.**

genetics approaches should be adopted to determine the number of true biological species and subsequent systematic studies should aim at identifying synapomorphies of these biological species and proposing new binomial names. *Mollugo nudicaulis* is similarly paraphyletic. In addition to a clade composed of accessions collected worldwide, two accessions from the Caribbean (Navassa Island and British Virgin Islands) formed a distinct clade separated from the other *M. nudicaulis* by several species (Fig. 3). Ekman determined the *M. nudicaulis* he collected on Navassa Island as *M. nudicaulis* var. *navassensis* (inscription on the herbarium sheet, Erik L. Ekman—10810, MO), a variety that might be raised to the species level in light of our results.

Finally, *M. verticillata* is also not monophyletic, with a clade sister to a Cuban species (*M. enneandra*) and a Bolivian accession sister to several species of the Galapagos islands, which present almost no variation in plastid markers (*M. crockerii*, *M. flavescens*, *M. flavescens* subsp. *insularis*, *M. floriana*, and *M. snodgrassii*). This complex, which will be referred to as the *verticillata* group, also requires fine-scale biogeographic and population genetics studies to determine species boundaries. Our initial results suggest that the cosmopolitan weed *M. verticillata* has produced divergent morphotypes; one in Cuba (*M. enneandra*), and several others after colonizing the Galapagos Islands. Wallace already hypothesized this evolutionary scenario for Galapagos *Mollugo* based on seed characters (Wallace 1987). The generation of significant morphological disparity without much apparent genetic divergence mirrors the diversification patterns of *Opuntia* in the Galapagos archipelago (Helsen et al. 2009).

The incongruence between molecular phylogenetics and taxonomy in the Molluginaceae questions the validity of using currently recognized species as evolutionarily relevant units in this group. We will consequently consider accessions as separate entities and use species names only as labels to describe groups of accessions.

MOLECULAR DATING

The split of Molluginaceae from their sister-group (Portulacineae) was estimated at 51.9 (±4.7) Mya and the first divergence within Molluginaceae at 46.7 (±4.8) Mya. The stem and crown nodes of the *verticillata* group were estimated at 13.4 (±4.2) Mya and 8.6 (±3.5) Mya, respectively. For the Galapagos endemics, stem and crown nodes were optimized at 4.3 (±2.1) and 3.0 (±1.6) Mya, respectively, which is congruent with the recent emergence of the Galapagos archipelago. The common ancestor of the *cerviana* and *fragilis* groups and *H. spergulacea* is estimated to have diverged from the *Pharnaceum*/*Adenogramma* clade 20.9 (±3.7) Mya. For the *cerviana* group, the stem and crown group ages were estimated at 9.6 (±2.7) and 2.0 (±1.1) Mya, respectively and for *fragilis*, at 7.2 (±2.2) and 1.9 (±0.9) Mya. The estimated 9.6 My of divergence between *cerviana* and *fragilis* groups supports the hypothesis that these represent different species. Similarly, *M. nudicaulis* var. *navassensis* and the other *M. nudicaulis* diverged 19.8 (±4.7) Mya, and likely do not belong to the same biological species.

The dating analyses produced very similar results when constraints were successively removed (Fig. S4), indicating no major conflict between the different calibration points. Removing the upper bound of 130 Mya on the crown of the eudicots and changing the maximal age for the root of the tree from 160 to 200 Mya strongly affected the estimate of the age of the root, as expected. However, estimates for Molluginaceae remained largely unchanged. In this analysis with relaxed upper limits, stem and crown of Molluginaceae were brought back to 56.1 (±5.8) and 50.3 (±5.8) Mya, respectively and the stem group nodes of *cerviana* and *fragilis* groups to 10.2 (±2.9) and 7.6 (±2.4) Mya, respectively. Thus, our conclusions remain largely unaffected by any uncertainty regarding the age of angiosperms.

LEAF ANATOMY

Although most of the dried leaf samples show some damage when fixed, it was still feasible to make out critical features pertaining to C_4 trait evolution, in particular, enlarged BSC, increased organelle density in BSC, aggregation of organelles along the inner BSC wall, and increased vein density such that the distance between mesophyll cells and BSC is reduced. Together, these features indicate C_3–C_4 intermediacy in species with a C_3 isotope ratio. *Mollugo pentaphylla* had a clear C_3 anatomy (Fig. 4A), whereas *M. verticillata* (C_3–C_4) exhibited a dense aggregation of plastids in slightly enlarged BSC (Fig. 4B), confirming its prior determination as a C_3–C_4 species (Kennedy and Laetsch 1974). *Mollugo nudicaulis* had large numbers of chloroplasts in BSC relative to typical C_3 plants (Fig. 4C), and has been previously physiologically shown to be a weak C_3–C_4 intermediate (Kennedy et al. 1980). Concentration of chloroplasts in BSC seem to be also present in its closest relatives (*M. decandra* and *M. nudicaulis* var. *navassensis*), although whether this is linked to C_3–C_4 physiology in these taxa remains to be assessed. In the clade of *Adenograma*/*Pharnaceum* that is immediately sister to the *M. cerviana* complex, BSC of three accessions that branch from the basal portion of the clade (*Suessenguthiella scleranthoides*, *Adenogramma sylvatica* and *M. tenella*) were enlarged compared to a typical C_3 pattern, but lacked any obvious enhancement of chloroplasts (Fig. S5). A species with narrow, linear leaves, *Pharnaceum detonsum,* did not have BSC that were enlarged from the C_3 condition (Fig. S5).

The leaf anatomy of *H. spergulacea* was similar to C_3–C_4 intermediates (Fig. 4D; McKown and Dengler 2007). Bundle sheaths were enlarged compared to *M. pentaphylla*, and showed a distinct aggregation of multiple organelles on the inner bundle

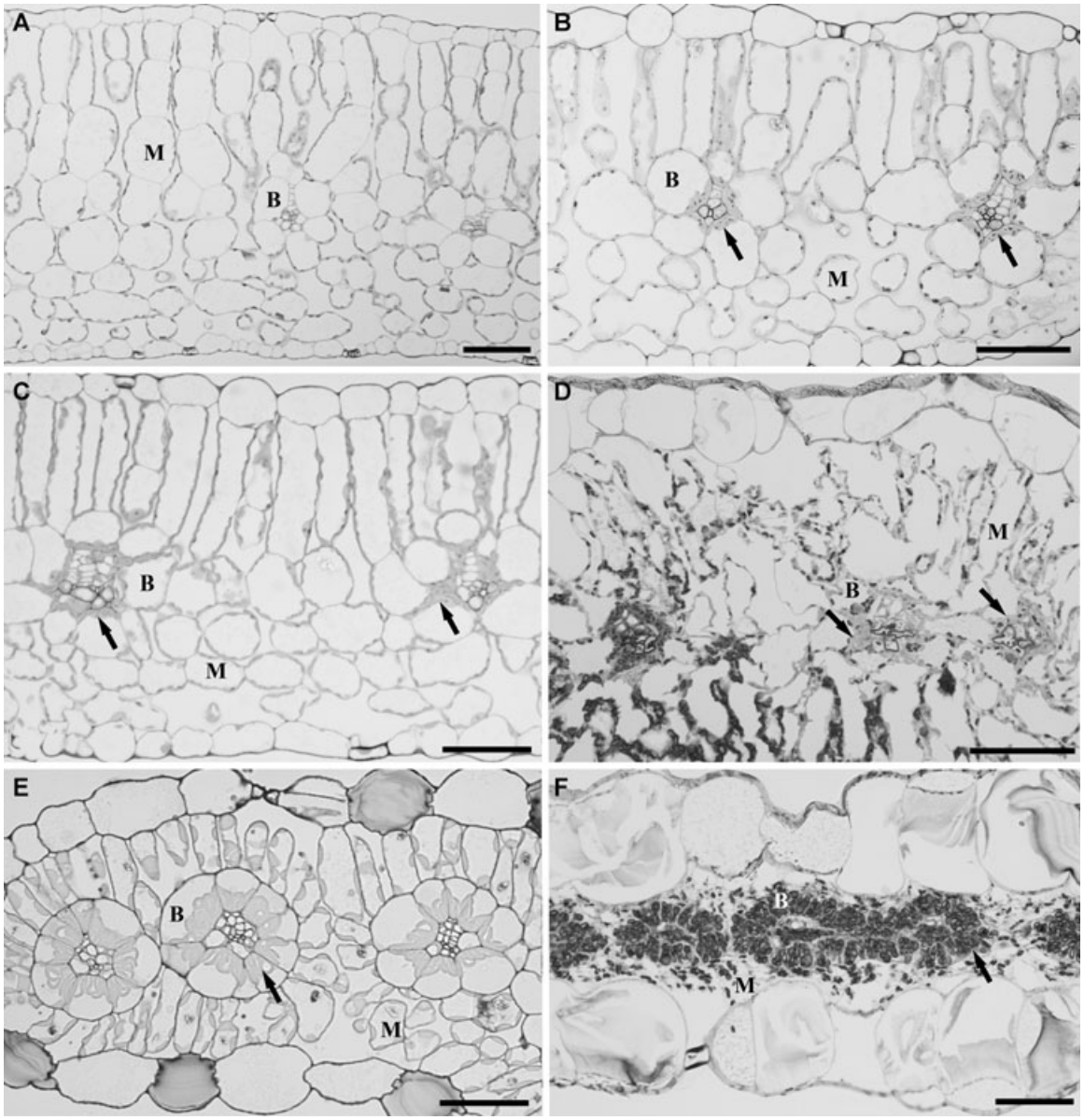

Figure 4. Light micrographs illustrating leaf anatomy of select Molluginaceae. (A) *Mollugo pentaphylla,* (B) *M. verticillata*, (C) *M. nudicaulis,* (D) *Hypertelis spergulacea,* (E) *M. cerviana, and* (F) *M. fragilis*. *Mollugo cerviana* and *M. fragilis* are C_4 species. Arrows highlight chloroplasts in the bundle sheath cells. B = bundle sheath; M = mesophyll. Bars = 50 μm.

sheath wall, as is widely observed in many C_3–C_4 species (Sage 2004). *Hypertelis spergulacea* also showed an increase in vein density to the degree that veins and BSC cells were separated by one to two mesophyll cells only (Fig. 4D). The accessions labeled *M. fragilis* and *M. cerviana* have a clearly C_4 leaf anatomy, assignable to the "Atriplicoid" type (Fig. 4E–F).

EVOLUTION OF GENES ENCODING PEPC

Two major *ppc* gene lineages exist in the core eudicots, *ppc-1* and *ppc-2* (Fig. S3). Eudicot *ppc* were highly supported as monophyletic and were sister to all monocot *ppc* genes, confirming that the diversification of *ppc* occurred after the eudicot–monocot split (Christin and Besnard 2009). The species relationships deduced from each of these gene lineages are congruent with the angiosperm phylogeny (APG III 2009).

Relationships among Molluginaceae taxa deduced from both *ppc-1* and *ppc-2* are compatible with plastid phylogenies (Fig. 5, Fig. S3). Genes encoding C_4-optimized PEPC are recognizable by their Ser at position 780, a residue that characterizes the sequenced C_4 *ppc*, but not non-C_4 *ppc,* in *Flaveria*, *Alternanthera* (Amaranthaceae), grasses, and sedges (Engelmann et al. 2003; Gowik et al. 2006; Christin et al. 2007; Besnard et al. 2009; Christin and Besnard 2009). C_4 *ppc* were only found in *cerviana* and *fragilis* groups and all belonged to the

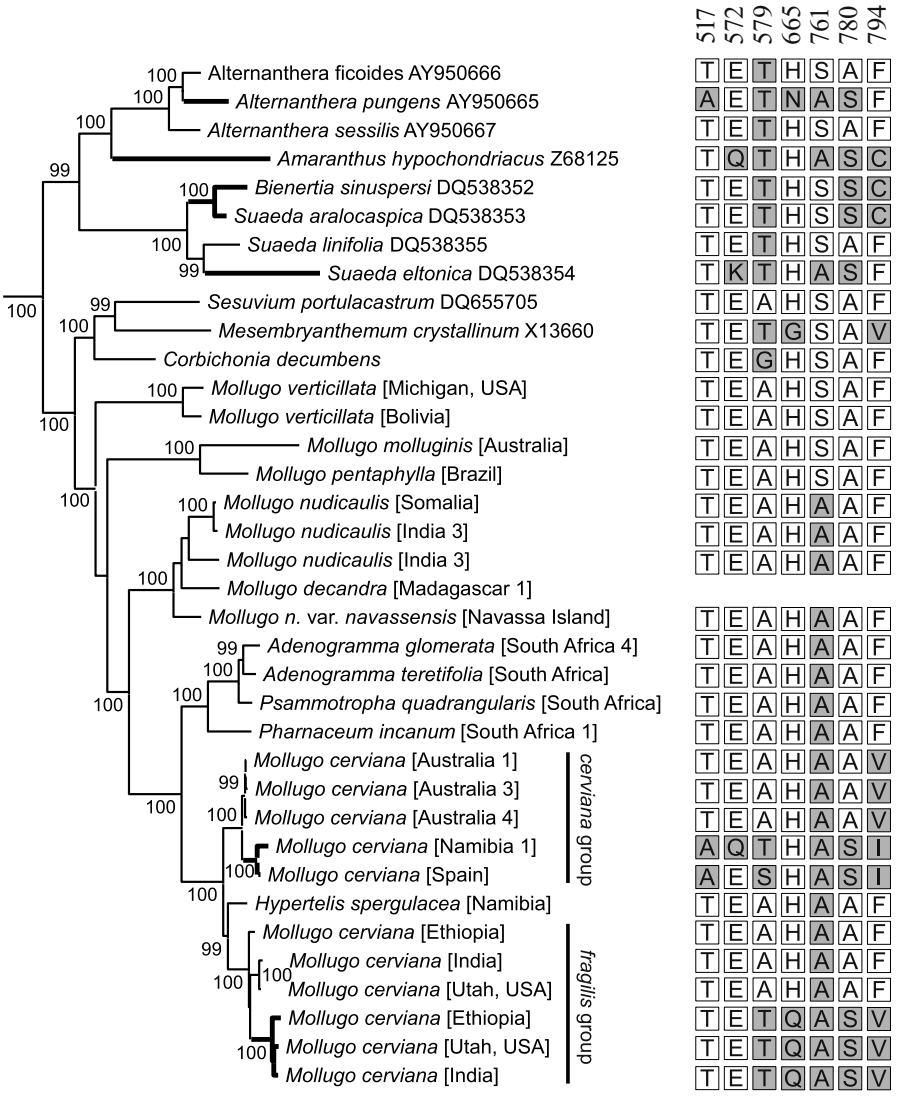

Figure 5. The evolutionary history of genes encoding PEPC in core Caryophyllales. This figure details the evolutionary history of Caryophyllales *ppc-1* lineage. Branches leading to C_4-specific genes, identified by a Serine at position 780, are in bold. Species names are followed by accession numbers for sequences retrieved from GenBank and geographic identifications for Molluginaceae. The numbering follows Figure 3 and Table S2. On the right, amino acid at positions shown to be under positive selection for the C_4 function in grasses (Christin et al. 2007) and which underwent similar changes in Caryophyllales are indicated. The amino acids at these positions are unknown for *M. decandra*, for which only a partial sequence was successfully isolated. Amino acids numbering is based on Zea mays PEPC (CAA33317). Residues that differ from the C_3 type are highlighted in gray.

ppc-1 gene lineage (Fig. 5). However, no *ppc* gene with the C_4-specific Ser780 were isolated from the Australian accessions of the *cerviana* group. Our PCR-mediated *ppc* survey could have missed the C_4-specific genes in these accessions because of mutations in the primer binding sites. More likely, these accessions use a PEPC that is competent but not optimized for the C_4 pathway, or is optimized by amino acids that differ from those currently known in other plant groups, such as Ser780. Detailed transcriptome analyses are needed to resolve this issue.

In addition to the Ser780, the *Mollugo* genes for C_4 PEPC present several amino acid changes compared to the non-C_4 sister genes that also appeared through independent adaptive changes in monocots and other eudicot C_4 lineages (Christin et al. 2007; Besnard et al. 2009). These amino acid substitutions are absent from related *ppc* genes from analyzed C_3 and C_3–C_4 intermediates in the Molluginaceae (Fig. 5). This reinforces the putative C_4 function of the genes with the Ser780, and confirms the occurrence of genetic convergence on wide taxonomic scales during C_4 PEPC evolution (Besnard et al. 2009). In the *fragilis* group, the *ppc-1* gene was duplicated after the divergence of this group from the *cerviana group* and only one of the duplicates possesses putatively C_4-adaptive amino acids (Fig. 5). In the *cerviana* group, many of

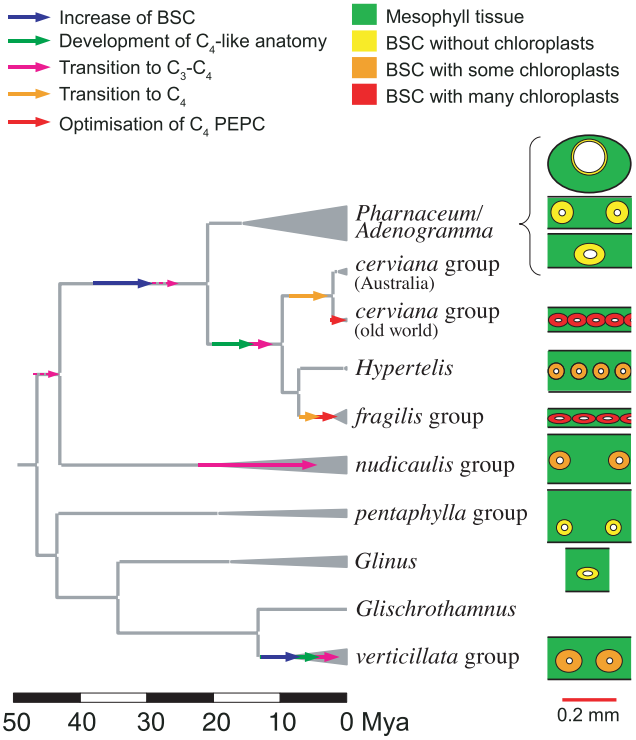

Figure 6. Gradual acquisitions of C_3–C_4 and C_4 photosynthesis. The major transitions that finally led to the emergence of C_4 photosynthesis are indicated by arrows on the calibrated phylogeny of Molluginaceae (see Fig. 3 for details). Dashed arrows indicate alternative scenarios. Diagrams of leaf anatomy (excluding epidermis) on the right are based on Figure 4 and Figure S5, except for *Glinus*, which is based on Kennedy et al. (1980). They are at the same scale, represented by the red bar at the bottom.

putative C_4-adaptive residues are present only in the accessions from South Africa and Spain (Fig. 5).

Discussion

MULTIPLE CO-OPTIONS OF C_3–C_4 TRAITS FOR C_4 EVOLUTION

In our survey, we found evidence of C_4 photosynthesis in only two genetic clusters of *Mollugo* accessions; the *cerviana* and *fragilis* groups (Fig. 3). Analyses of genes encoding PEPC showed that the optimization of this C_4 key enzyme of the *cerviana* group followed a gene duplication event that occurred after the divergence from the *fragilis* group, which demonstrates two independent optimizations of C_4 biochemistry in these closely related taxa during the last 10 Mya (Fig. 6). Moreover, C_4-characteristic amino acids were acquired in some accessions of the *fragilis* groups after the divergence of the Australian line (Fig. 5), and a few variations exist at these sites between South African and Spanish *cerviana* accessions. This indicates that fine tuning of C_4 biochemistry took place in this group within the last million years, after the emergence of a functional C_4 pathway (Fig. 6). This also shows that a relatively high number of adaptive amino acid replacements can be fixed in a short period of time.

Hypertelis spergulacea, which separates the two C_4 groups in plastid and nuclear phylogenies (Figs. 3 and 5), is C_3–C_4 based on structural traits that characterize well-developed C_3–C_4 species (Fig. 4D; Monson and Rawsthorne 2000; Sage 2004; McKown and Dengler 2007; Voznesenskaya et al. 2007). The common ancestor of the two C_4 groups and *H. spergulacea* thus likely also exhibited structural characters intermediate between the C_3 and C_4 conditions and used an intermediate photosynthetic pathway. These morphological and physiological attributes were independently co-opted in the evolution of full C_4 syndromes in the *cerviana* and *fragilis* lineages. Similar co-options of C_3–C_4 traits are thought to have occurred during C_4 evolution within other C_4 groups (Monson and Rawsthorne 2000; Marshall et al. 2007; McKown and Dengler 2007). In C_3–C_4 intermediates, CO_2 released in photorespiration is localized to the BSC due to a loss of glycine decarboxylase (GDC) expression in the mesophyll tissue (Hylton et al. 1988; Monson and Moore 1989; Monson and Rawsthorne 2000). This concentrates CO_2 around Rubisco in the BSC and suppresses photorespiration (von Caemmerer 1992). Models of C_4 evolution developed from *Flaveria* predict that exploitation of CO_2 release by BSC-localized GDC promotes an expansion of the BSC and an increase of the number of chloroplasts and mitochondria in the BSC, and leads to the establishment of efficient flux networks to rapidly move photorespiratory metabolites between BSC and mesophyll tissues (Monson and Rawsthorne 2000; Sage 2004). Thus, many of the C_4 traits are preestablished in the C_3–C_4 intermediates, and this may facilitate multiple spin-offs of C_4 species.

ANATOMICAL PRECONDITIONS FOR C_3–C_4 PHOTOSYNTHESIS

Several species from the sister group to the *cerviana/fragilis/H. spergulacea* complex have enlarged BSC and reduced interveinal distance compared to C_3 taxa (Fig. S5). The distribution of enlarged BSC in the phylogeny (Figs. 3 and 6) suggests that this character appeared more than 20 Mya at the base of the clade containing the C_4 groups, *H. spergulacea* and the *Adenogramma/Pharnaceum* group (Fig. 6). This could be linked with C_3–C_4 photosynthesis, but the absence of organelle clusters in the BSC of *Suessenguthiella*, *Adenogramma*, *Pharnaceum* and *M. tenella* does not support this hypothesis. Enlarged BSC probably evolved in a C_3 context, perhaps to act as hydraulic capacitors to buffer sudden surges in transpiration in a hot, windy environment (Sage 2001, 2004). This character was likely co-opted to evolve the C_3–C_4 type that was further used for the C_4 pathway of the *cerviana* and *fragilis* groups. Thus, enlarged BSC probably represent developmental enablers sensu Donoghue (2005).

The presence of enlarged BSC and close vein spacing reduces the chance that a knockout of mesophyll GDC expression is lethal, simply by reducing the distance between mesophyll and BSC and thus allowing for sufficiently rapid transport of photorespiratory metabolites to the BSC. Similar anatomical traits may have increased the probability of transition to C_3–C_4 photosynthesis in other lineages where the C_4 pathway evolved (McKown and Dengler 2007; Marshall et al. 2007; Muhaidat 2007; Muhaidat et al. 2007).

The distribution of anatomical characters, adaptive amino acid mutations, and functional characters in Molluginaceae phylogeny presents a scenario in which characteristics associated with C_4 photosynthesis, such as increased BSC, emerged in a C_3 or a moderate C_3–C_4 context. Successive speciation and migration events presented the plants with new environmental pressures that promoted the emergence of C_4-like anatomy in some lineages, probably linked with the development of a C_3–C_4 biochemistry. These successive co-options of preconditioning characters followed by fine-tuning of the C_4 biochemistry, spread over several million years, finally gave rise to widespread, ecologically successful C_4 taxa.

C_3–C_4 INTERMEDIACY AS AN ADAPTIVE STRATEGY

Characters of C_3–C_4 intermediacy appeared at least twice in the Molluginaceae. *Mollugo verticillata* is positioned within a clade of C_3 species, and this taxon is not closely related to any C_4 taxon or C_3–C_4 intermediates, having diverged from the *M. cerviana* and *M. nudicaulis* groups more than 40 Mya. C_3–C_4 photosynthesis also evolved in the clade encompassing *M. nudicaulis* and *H. spergulacea*, but it is difficult to determine the exact number of C_3–C_4 origins in this group. This would require alternative approaches such as comparing the genes controlling specific C_3–C_4 characteristics (Christin et al. 2010). A C_3–C_4 type without enlarged BSC could have appeared in their common ancestors and a more pronounced C_4-like leaf anatomy may have subsequently evolved in the lineage leading to the *cerviana/fragilis* groups and *H. spergulacea*. An alternative scenario would imply two independent origins of C_3–C_4 intermediacy, one in the *nudicaulis* group and one in the lineage leading to *cerviana-fragilis-H. spergulacea* group. This would explain why *H. spergulacea* and *M. nudicaulis* have C_3–C_4 characteristics that are anatomically distinct.

C_3–C_4 photosynthesis is believed to be a relatively rare condition in plants, with only a few dozen identified species, many of which belong to *Flaveria* (Sage et al. 1999). Most C_3–C_4 lineages have only one or two species, and these tend to have restricted distributions, both geographically and in terms of habitat (Frohlich 1978; Powell 1978; Sage et al. 1999). Of all the C_3–C_4 intermediates, *M. nudicaulis* and *M. verticillata* are the most widespread and abundant. Both are found in hot, ruderal habitats where competition is low and the potential for photorespiration is high. Their ability to survive on such sites is likely due to their C_3–C_4 pathway, which improves carbon gain in the reduced atmospheric CO_2 levels that were prevalent in recent geological time (Vogan et al. 2007). The ecological success of these C_3–C_4 *Mollugo* demonstrates that C_3–C_4 intermediacy has to be considered as a successful photosynthetic pathway in its own right and not merely a transitional phase to C_4 photosynthesis. If all members of the *verticillata* and *nudicaulis* groups are C_3–C_4, then our results indicate C_3–C_4 intermediacy is older than 8.6 and 19.8 My in these two groups, respectively. Intermediate traits between C_3 and C_4 were also estimated to be older than 10 Mya in the lineage that gave birth to *H. spergulacea* (Fig. 6). This evolutionary stability increases the probability that some descendants would fix mutations toward more C_4-like characteristics and thus increases the chances of C_4 photosynthesis evolving in certain clades.

GLOBAL ECOLOGICAL DRIVERS OF C_4 EVOLUTION AND THE MOLLUGINACEAE

The earliest C_4 origins are estimated to have occurred in the grasses about the time atmospheric CO_2 levels fell to near current levels (32–25 Mya), an event that created the primary environmental requirement for C_4 evolution in terrestrial plants (Christin et al. 2008). Other C_4 clades in grasses, sedges and Amaranthaceae appeared over the subsequent 20 My (Kadereit et al. 2003; Christin et al. 2008; Besnard et al. 2009). Our dating results indicate C_3–C_4 and C_4 photosynthesis in the Molluginaceae also appeared during this period. Although it is currently difficult to place the geographic location for the origins of C_4 photosynthesis in the *cerviana* and *fragilis* clades, it is plausible to hypothesize that in both the *cerviana* and *fragilis* clades, the C_4 pathway arose in southwestern Africa. This hypothesis is supported by the restriction of *H. spergulacea* and the *Adenogramma*/*Pharnaceum* clade to this area (Riley 1963; African Plant Database 2010). Many Molluginaceae of this region grow in sandy soils, in climates characterized by very hot summers with some monsoon precipitation (African Plant Database 2010). Because of the episodic monsoon rains, summer photosynthesis by ephemeral species is possible on sandy soils where vegetation cover is sparse and soil moisture is readily available for brief periods. However, temperatures near the soil surface are very hot (>40°C typically) and photorespiration rates in C_3 species would be extreme, particularly in the low CO_2 atmospheres of the past 30 Mya. It seems likely that the sandy soils of southern Africa, coupled with extreme conditions of very high temperatures and low atmospheric CO_2, provided a strong selection pressure for carbon conservation mechanisms that, through successive transitional stages, ultimately led to two C_4 lineages in the Molluginaceae.

Conclusion

In this study, we have shown that C_3–C_4 photosynthesis evolved at least twice and possibly three times in the Molluginaceae, with two subsequent transitions to fully developed C_4 photosynthesis. This multiplicity of photosynthetic transitions is remarkable given that both C_3–C_4 intermediacy and C_4 photosynthesis are complex traits that require important genetic modifications. Initial transitions to C_3–C_4 were facilitated by anatomical traits present in the C_3 ancestors, whereas the C_4 pathway in two closely related lineages emerged through co-option of C_3–C_4 characters present in their common ancestor. The *cerviana* and *fragilis* C_4 groups likely made the transition to a fully functional C_4 pathway independently, but they acquired their C_4 anatomy from their common ancestor. Similarly, the optimization of the C_4 biochemistry occurred independently in geographically isolated members of the *cerviana* group, although they likely inherited a functional C_4 trait from the same ancestor. Thus, although the optimization of the C_4 biochemistry occurred within the last million years in the *cerviana* group, the full transition from a typical C_3 ancestor to a fully C_4 plant was probably spread across more than 20 million years (Fig. 6). Acknowledging that many apparent "multiple origins" of the C_4 trait are in reality only partially independent can contribute to understanding the apparent paradox between the high number of C_4 lineages and the genetic complexity of the C_4 trait. Rather than considering C_3 and C_4 photosynthesis as discrete, binary traits, evolutionary studies should consider the probability of developing anatomical characters suitable for a more C_4-like condition and then, given the presence of such facilitators, the probability of transition toward a more C_4-like state. Such considerations would likely confirm that C_4 photosynthesis, as a complex trait, is unlikely to evolve in a randomly selected plant lineage. Instead, the possibility of co-opting anatomical or biochemical traits preexisting in certain groups, and the evolutionary stability of C_3–C_4 intermediates, can strongly increase the probability of some lineages acquiring C_4 photosynthesis. Given this understanding, it is apparent that the study of C_4 evolution should examine in detail the traits of the C_3 plants related to C_4 taxa, to identify when and why critical developmental enablers for C_4 first appeared.

ACKNOWLEDGMENTS

This study was partially funded by the Swiss National Science Foundation grant PBLAP3-129423 to PAC, NSERC Discovery grants to RFS and TLS, and National Science Foundation grants IOS-0843231 and DEB-1026611 to EJE. The authors are extremely thankful to the New York Botanical Garden, the Royal Botanical gardens of Kew, the Australian National Herbarium (CANB), the herbarium of the Royal Botanical gardens at Sydney, New South Wales (NSW), the herbarium of the University of Sao Paulo, Brazil (SPF), the Herbarium of the conservatory and botanical garden of the City of Geneva and the Herbarium Senckenbergianum at Frankfurt for providing the necessary plant samples and providing their expertise. We are particularly thankful for the assistance of M. Thulin of the University of Uppsala, M. Chase and E. Kapinos at Kew gardens, L. Gautier and N. Fumeaux at Geneva, and J. Palmer at CANB who provided herbarium samples. We also thank the Compton Herbarium (NBG) at Kirstenbosch for providing material support during a collecting trip in South Africa. We thank D. Hansen for assistance with the fixation of herbarium specimens. We also thank M. Arakaki, G. Besnard, L. Buchi, D. Chatelet, N. Salamin, E. Samaritani, K. Schmandt, and S. Schmerler for helpful discussions and comments on earlier versions of the manuscript.

LITERATURE CITED

Adoutte, A., G. Balavoine, N. Lartillot, and R. de Rosa. 1999. Animal evolution—the end of the intermediate taxa? Trends Genet. 15:104–108.

African Plants Database. 2010. Version 3.3. Conservatoire et Jardin botaniques de la Villle de Genève and South African National Biodiversity Institute, Pretoria. Available at http://www.ville-ge.ch/musinfo/bd/cjb/africa. Accessed May 18, 2010.

APG III. 2009. An update of the Angiosperm Phylogeny Group classification for the orders and families of flowering plants: APG III. Bot. J. Linn. Soc. 161:105–121.

Besnard, G., A. M. Muasya, F. Russier, E. H. Roalson, N. Salamin, and P. A. Christin. 2009. Phylogenomics of C_4 photosynthesis in sedges (Cypercaeae): multiple appearances and genetic convergence. Mol. Biol. Evol. 26:1909–1919.

Bläsing, O. E., P. Westhoff, and P. Svensson. 2000. Evolution of C_4 phospho*enol*pyruvate carboxylase in *Flaveria*, a conserved serine residue in the carboxyl-terminal part of the enzyme is a major determinant for C_4-specific characteristics. J. Biol. Chem. 275:27917–27923.

Brockington, S. F., R. Alexandre, J. Ramdial, M. J. Moore, S. Crawley, A. Dhingra, K. Hilu, D. E. Soltis, and P. S. Soltis. 2009. Phylogeny of the Caryophyllales sensu lato: revisiting hypotheses on pollinations biology and perianth differentiation in the core Caryophyllales. Int. J. Plant Sci. 170:627–643.

Chastain, C. 2011. Structure, function, and post-translational regulation of C_4 pyruvate orthophosphate dikinase. Pp. 301–315 *in* A. S. Raghavendra and R. F. Sage, eds. C_4 photosynthesis and related CO_2 concentrating mechanisms. Springer Verlag, Berlin, Germany.

Cho, Y., J. P. Mower, Y. L. Qiu, and J. D. Palmer. 2004. Mitochondrial substitution rates are extraordinarily elevated and variable in a genus of flowering plants. Proc. Natl. Acad. Sci. USA 101:17741–17746.

Christin, P. A., and G. Besnard. 2009. Two independent C_4 origins in Aristidoideae (Poaceae) revealed by the recruitment of distinct phosphoenolpyruvate carboxylase genes. Am. J. Bot. 96:2234–2239.

Christin, P. A., N. Salamin, V. Savolainen, M. R. Duvall, and G. Besnard. 2007. C_4 photosynthesis evolved in grasses via parallel adaptive genetic changes. Curr. Biol. 17:1241–1247.

Christin, P. A., G. Besnard, E. Samaritani, M. R. Duvall, T. R. Hodkinson, V. Savolainen, and N. Salamin. 2008. Oligocene CO_2 decline promoted C_4 photosynthesis in grasses. Curr. Biol. 18:37–43.

Christin, P. A., R. P. Freckleton, and C. P. Osborne. 2010. Can phylogenetics indentify C_4 origins and reversals? Trends Ecol. Evol. 25:403–409.

Combes, C. 2001. Les associations du vivant: L'art d'être parasite. Flammarion, Paris, France.

Cuénoud, P., V. Savolainen, L. W. Chatrou, M. Powell, R. J. Grayer, and M. W. Chase. 2002. Molecular phylogenetics of Caryophyllales based on nuclear 18S rDNA and plastid *rbcL*, *atpB*, and *matK* DNA sequences. Am. J. Bot. 89:132–144.

Donoghue, M. J. 2005. Key innovations, convergence, and success: macroevolutionary lessons from plant phylogeny. Palaebiology 31:77–93.

Ehleringer, J. R., T. E. Cerling, and B. R. Helliker. 1997. C_4 photosynthesis, atmospheric CO_2 and climate. Oecologia 112:285–299.

Endress, M. E., and V. Bittrich. 1993. Molluginaceae. Pp. 419–426 *in* K. Kubitzki, J. G. Rohwer, and V. Bittrich, eds. The families and genera of vascular plants, vol. II, Magnoliid, hamamelid, and caryophyllid families. Springer Verlag, Berlin, Germany.

Engelmann, S., O. E. Bläsing, U. Gowik, P. Svensson, and P. Westhoff. 2003. Molecular evolution of C_4 phosphoenolpyruvate carboxylase in the genus *Flaveria*-–a gradual increase from C_3 to C_4 characteristics. Planta 217:717–725.

Friis, E. M., K. Raunsgaard Pedersen, and P. R. Crane. 2006. Cretaceous angiosperm flowers: innovation and evolution in plant reproduction. Palaeogeogr. Palaeoclimatol. Palaeoecol. 232:251–293.

Frohlich, M. W. 1978. Systematics of *Heliotropium* section *Orthostachys* in Mexico. Ph.D. dissertation. Harvard University, Cambridge, MA.

Gowik, U., S. Engelmann, O. E. Bläsing, A. S. Raghavendra, and P. Westhoff. 2006. Evolution of C_4 phosphoenolpyruvate carboxylase in the genus *Alternanthera*: gene families and the enzymatic characteristics of the C_4 isozyme and its orthologues in C_3 and C_3/C_4 *Alternantheras*. Planta 223:359–368.

Griffiths, H. 1989. Carbon dioxide concentrating mechanisms in relation to the evolution of CAM in vascular epiphytes. Pp. 42–86 *in* U. Luttge, ed. Ecological studies 76: vascular plants as epiphytes. Springer Verlag, Berlin, Germany.

Hattersley, P. W., S. C. Wong, S. Perry, and Z. Roksandic. 1986. Comparative ultrastructure and gas-exchange characteristics of the C_3–C_4 intermediate *Neurachne minor*. Plant Cell Environ. 9:217–233.

Helsen, P., R. A. Browne, D. J. Anderson, P. Verdyck, and S. Dongen. 2009. Galapagos' *Opuntia* (prickly pear) cacti: extensive morphological diversity, low genetic variability. Biol. J. Linn. Soc. 96:451–461.

Herron, M. D., and R. E. Michod. 2008. Evolution of complexity in the volvocine algae: transitions in individuality through Darwin's eye. Evolution 62:436–451.

Hibberd, J. M., and S. Covshoff. 2010. The regulation of gene expression required for C_4 photosynthesis. Annu. Rev. Plant Biol. 61:181–207.

Hylton, C. M., S. Rawsthorne, A. M. Smoth, and D. A. Jones. 1988. Glycine decarboxylase is confined to the bundle-sheath cells of leaves of C_3–C_4 intermediate species. Planta 175:452–459.

Jacobs, B., S. Engelmann, P. Westhoff, and U. Gowik. 2008. Evolution of C_4 phospho*enol*pyruvate carboxylase in *Flaveria*: determinants for high tolerance towards the inhibitor L-malate. Plant Cell Environ. 31:793–803.

Jordan, G. J., and M. K. Mcphail. 2003. A middle-late Eocene inflorescence of Caryophyllaceae from Tasmania, Australia. Am. J. Bot. 90:761–768.

Kadereit, G., T. Borsch, K. Weising, and H. Freitag. 2003. Phylogeny of Amaranthaceae and Chenopodiaceae and the evolution of C_4 photosynthesis. Int. J. Plant Sci. 164:959–986.

Kennedy, R. A., and W. M. Laetsch. 1974. Plant species intermediate for C_3, C_4 photosynthesis. Science 184:1087–1089.

Kennedy, R. A., J. L. Eastburn, and K. G. Jensen. 1980. C_3–C_4 photosynthesis in the genus *Mollugo*: structure, physiology and evolution of intermediate characteristics. Am. J. Bot. 67:1207–1217.

Kishino, H., J. L. Thorne, and W. J. Bruno. 2001. Performance of a divergence time estimation method under a probabilistic model of rate evolution. Mol. Biol. Evol. 18:352–361.

Ku, M. S. B., J. R. Wu, Z. Y. Dai, R. A. Scott, C. Chu, and G. E. Edwards. 1991. Photosynthetic and photorespiratory characteristics of *Flaveria* species. Plant Physiol. 96:518–528.

Ku, M. S. B., Y. KanoMurakami, and M. Matsuoka. 1996. Evolution and expression of C_4 photosynthesis genes. Plant Physiol. 111:949–957.

Lamb, T. D., S. P. Collin, and E. N. Pugh. 2007. Evolution of the vertebrate eye: opsins, photoreceptors, retina and eye cup. Nat. Rev. Neurosci. 8:960–975.

Leegood, R. C., and R. P. Walker. 1999. Regulation of the C_4 pathway. Pp. 89–131 *in* R. F. Sage and R. K. Monson, eds. C_4 Plant biology. Academic Press, San Diego, CA.

Leegood, R. C. 2008. Roles of the bundle sheath cells in leaves of C_3 plants. J. Exp. Bot. 59:1663–1673.

Magallon, S., and M. J. Sanderson. 2001. Absolute diversification rates in angiosperm clades. Evolution 55:1762–1780.

Marshall, D. M., R. Muhaidat, N. J. Brown, Z. Liu, S. Stanley, H. Griffiths, R. F. Sage, and J. M. Hibberd. 2007. *Cleome*, a genus closely related to *Arabidopsis*, contains species spanning a developmental progression from C_3 to C_4 photosynthesis. Plant J. 51:886–896.

McKown, A. D., and N. G. Dengler. 2007. Key innovations in the evolution of Kranz anatomy and C_4 vein pattern in *Flaveria* (Asteraceae). Am. J. Bot. 94:382–399.

McKown, A. D., J. M. Moncalvo, and N. G. Dengler. 2005. Phylogeny of *Flaveria* (Asteraceae) and inference of C_4 photosynthesis evolution. Am. J. Bot. 92:1911–1928.

Monson, R. K. 1999. The origins of C_4 genes and evolutionary pattern in the C_4 metabolic phenotype. Pp. 377–410 *in* R. F. Sage and R. K. Monson, eds. C_4 Plant biology. Academic Press, San Diego, CA.

Monson, R. K., and B. D. Moore. 1989. On the significance of C_3–C_4 intermediate photosynthesis to the evolution of C_4 photosynthesis. Plant Cell Environ. 12:689–699.

Monson, R. K., and S. Rawsthorne. 2000. CO_2 assimilation in C_3–C_4 intermediate plants. Pp. 533–550 *in* R. C. Leegood, T. D. Sharkey, and S. von Caemmerer, eds. Photosynthesis: physiology and metabolism. Kluwer Academic Publishers. Dordrecht. The Netherlands.

Muhaidat, R. 2007. Diversification of C_4 photosynthesis in the eudicots: anatomical, biochemical and physiological perspectives. Ph.D. dissertation, University of Toronto, Toronto, Ontario, Canada. 236 pp.

Muhaidat, R., R. F. Sage, and N. G. Dengler. 2007. Diversity of Kranz anatomy and biochemistry in C_4 eudicots. Am. J. Bot. 94:362–381.

Nakamoto, H., M. S. B. Ku, and G. E. Edwards. 1983. Photosynthetic characteristics of C_3–C_4 intermediate *Flaveria* species II. Kinetic properties of phosphoenopyruvate carboxylase from C_3, C_4 and C_3–C_4 intermediate species. Plant Cell Physiol. 24:1387–1393.

Nyffeler, R., and U. Eggli. 2010. Desintegrating Portulaceae: a new familial classification of the suborder Portulacineae (Caryophyllales) based on molecular and morphological data. Taxon 59:227–240.

Nyffeler, R., U. Eggli, M. Ogburn, and E. J. Edwards. 2008. Variations on a theme: repeated evolution of succulent life forms in the Portulacineae (Caryophyllales). Haseltonia 14:26–36.

O'Brien, T. P., and M. E. McCully. 1981. The study of plant structure: principles and selected methods. Termarcarphi, Victoria, Australia.

Ogawa, A., A. Streit, A. Antebi, and R. J. Sommer. 2009. A conserved endocrine mechanism controls the formation of dauer and infective larvae in nematodes. Curr. Biol. 19:67–71.

Parkinson, C. L., J. P. Mower, Y. L. Qiu, A. J. Shirk, K. Song, N. D. Young, C. W. dePamphilis, and J. D. Palmer. 2005. Multiple major increases and decreases in mitochondrial substitution rates in the plant family Geraniaceae. BMC Evol. Biol. 5:73.

Powell, A. M. 1978. Systematics of *Flaveria* (Flaveriinae-Asteraceae). Ann. Mo. Bot. Gard. 65:590–636.

Rajendru, G., J. S. R. Prasad, and V. S. R. Das. 1986. C_3–C_4 intermediate species in *Alternanthera* (Amaranthaceae). Plant Physiol. 80:409–414.

Riley, H. P. 1963. Families of flowering plants of southern Africa. Univ. of Kentucky Press, Lexington, KY, 269 pp.

Ronquist, F., and J. P. Huelsenbeck. 2003. MrBayes 3: Bayesian phylogenetic inference under mixed models. Bioinformatics 19:1572–1574.

Rutschmann, F. 2006. Molecular dating of phylogenetic trees: a brief review of current methods that estimate divergence times. Divers. Distrib. 12:35–48.

Sage, R. F. 2001. Environmental and evolutionary preconditions for the origin and diversification of the C_4 photosynthetic syndrome. Plant Biol. 3:202–213.

———. 2004. The evolution of C_4 photosynthesis. New Phytol. 161:341–370.

Sage, T. L., and E. G. Williams. 1995. Structure, ultrastructure, and histochemistry of the pollen-tube pathway in the milkweed *Asclepias exaltata L.* Sex Plant Reprod. 8:257–265.

Sage, R. F., M. Li, and R. K. Monson. 1999. The taxonomic distribution of C_4 photosynthesis. Pp. 551–584 *in* R. F. Sage and R. K. Monson, eds. C_4 Plant biology. Academic Press, San Diego, CA.

Sawers, J. H., P. Liu, K. Anufrikova, J. G. Gene Hwang, and T. P. Brutnell. 2007. A multi-treatment experimental system to examine photosynthetic differentiation in the maize leaf. BMC Genomics 8:12.

Sayre, R. T., and R. A. Kennedy. 1979. Photosynthetic enzyme activities and localization in *Mollugo verticillata* populations differing in the levels of C_3 and C_4 cycle operation. Plant Physiol. 64:293–299.

Smith, S. A., J. M. Beaulieu, and M. J. Donoghue. 2010. An uncorrelated relaxed-clock analysis suggests an earlier origin of flowering plants. Proc. Natl. Acad. Sci. USA 107:5897–5902.

Spurr, A. R. 1969. A low-viscosity epoxy resin embedding medium for electron microscopy. J. Ultrastruct. Res. 26:31–43.

Svensson, P., O. E. Bläsing, and P. Westhoff. 2003. Evolution of C_4 phospho*enol*pyruvate carboxylase. Arch. Biochem. Biophys. 414:180–188.

Thorne, J. L., and H. Kishino. 2002. Divergence time and evolutionary rate estimation with multilocus data. Syst. Biol. 51:689–702.

Thorne, J. L., H. Kishino, and I. S. Painter. 1998. Estimating the rate of evolution of the rate of molecular evolution. Mol. Biol. Evol. 15:1647–1657.

Thompson, J. D., D. J. Higgins, and T. J. Gibson. 1994. ClustalW: improving the sensitivity of progressive multiple sequence alignment through sequence weighting, position specific gap penalties and matrix choice. Nucleic Acids Res. 22:4673–4680.

Tropicos. 2010. Tropicos.org. Missouri Botanical Garden. Available at http://www.tropicos.org. Accessed May 18, 2010.

Vincent, M. A. 2003. Molluginaceae Rafinesque. Pp. 509–512 *in* Flora of North America Editorial Committee. Flora of North America, volume 4: Magnoliophyta: Caryophyllidae, part 1. Oxford Univ. Press, Oxford, UK.

Vogan, P. J., M. W. Frohlich, and R. F. Sage. 2007. The functional significance of C_3–C_4 intermediate traits in *Heliotiopium* L. (Boraginaceae): gas exchange perspectives. Plant Cell Environ. 30:1337–1345.

von Caemmerer, S. 1992. Stable carbon isotope discrimination in C_3–C_4 intermediates. Plant Cell Environ. 15:1063–1072.

Voznesenskaya, E. V., N. K. Koteyeva, S. D. X. Chuong, A. N. Ivanova, J. Barroca, L. D. Craven, and G. E. Edwards. 2007. Physiological, anatomical, and biochemical characterization of photosynthetic types in genus *Cleome* (Cleomeaceae). Funct. Plant Biol. 34:247–267.

Wallace, R. S. 1987. Seed characters, biogeography, and systematics of the genus *Mollugo* (Molluginaceae). Am. J. Bot. 74:763–763.

Yang, Z. H. 2007. PAML 4: Phylogenetic analysis by maximum likelihood. Mol. Biol. Evol. 24:1586–1591.

Associate Editor: J. Vamosi

Supporting Information

The following supporting information is available for this article:

Figure S1. Primers used to PCR-amplify the *trnK-matK* marker.
Figure S2. The frequency distribution of carbon isotope ratios in the Molluginaceae sensu lato.
Figure S3: Detail of PEPC phylogeny.
Figure S4: Effect of removing calibration points on dating analyses.
Figure S5. Light micrographs of Molluginaceae.
Table S1. Carbon isotope ratios of accessions used in this study.
Table S2. Caryophyllales accessions and markers used in phylogenetic analyses.
Table S3. Taxa sampled for phylogenetic analyses outside Caryophyllales.
Table S4. List of *ppc* sequences generated in this study.

Supporting Information may be found in the online version of this article.

Please note: Wiley-Blackwell is not responsible for the content or functionality of any supporting information supplied by the authors. Any queries (other than missing material) should be directed to the corresponding author for the article.